Featured Article

Hypoxia and Glucose Metabolism in Malignant Tumors: Evaluation by [^{18}F]Fluoromisonidazole and [^{18}F]Fluorodeoxyglucose Positron Emission Tomography Imaging

Joseph G. Rajendran,[1,5] David A. Mankoff,[1] Finbarr O'Sullivan,[7] Lanell M. Peterson,[1] David L. Schwartz,[5,6] Ernest U. Conrad,[2] Alexander M. Spence,[3] Mark Muzi,[1] D. Greg Farwell,[4] and Kenneth A. Krohn[1,5]

Departments of [1]Radiology,[2]Orthopedic Surgery,[3]Neurology, [4]Otolaryngology, and [5]Radiation Oncology, University of Washington, Seattle, Washington; [6]Department of Radiation Oncology, Veterans' Administration Puget Sound Health Care System, Seattle, Washington; and [7]University College, Cork, Ireland

Abstract

Purpose: **The aim of this study is to compare glucose metabolism and hypoxia in four different tumor types using positron emission tomography (PET). ^{18}F-labeled fluorodeoxyglucose (FDG) evaluates energy metabolism, whereas the uptake of ^{18}F-labeled fluoromisonidazole (FMISO) is proportional to tissue hypoxia. Although acute hypoxia results in accelerated glycolysis, cellular metabolism is slowed in chronic hypoxia, prompting us to look for discordance between FMISO and FDG uptake.**

Experimental Design: **Forty-nine patients (26 with head and neck cancer, 11 with soft tissue sarcoma, 7 with breast cancer, and 5 with glioblastoma multiforme) who had both FMISO and FDG PET scans as part of research protocols through February 2003 were included in this study. The maximum standardized uptake value was used to depict FDG uptake, and hypoxic volume and maximum tissue: blood ratio were used to quantify hypoxia. Pixel-by-pixel correlation of radiotracer uptake was performed on coregistered images for each corresponding tumor plane.**

Results: **Hypoxia was detected in all four patient groups. The mean correlation coefficients between FMISO and FDG uptake were 0.62 for head and neck cancer, 0.47 for breast cancer, 0.38 for glioblastoma multiforme, and 0.32 for soft tissue sarcoma. The correlation between the overall tumor maximum standardized uptake value for FDG and hypoxic volume was small (Spearman $r = 0.24$), with highly significant differences among the different tumor types ($P < 0.005$).**

Conclusions: **Hypoxia is a general factor affecting glucose metabolism; however, some hypoxic tumors can have modest glucose metabolism, whereas some highly metabolic tumors are not hypoxic, showing discordance in tracer uptake that can be tumor type specific.**

Introduction

Solid tumors develop regions of hypoxia when they outgrow their blood supply. Distribution of oxygen within a tumor usually shows a gradient, diminishing toward the less vascularized center of the tumor (1, 2). Hypoxia induces an aggressive phenotype, increasing metastatic potential, promoting tumor progression, and limiting the effectiveness of radiation therapy and some chemotherapeutic agents (3, 4). These characteristics are related to induction of a number of biological changes that include angiogenesis, *p53* mutation, and altered regulation of cellular proliferation and glucose metabolism (5). Most solid cancer types can give rise to hypoxic regions. Significant (radiobiological) hypoxia has been detected in nearly 40% of patients with head and neck cancer (6–8). Several studies have shown smaller but significant levels of hypoxia in soft tissue sarcomas (9, 10), breast cancer (11, 12), and glioblastoma multiforme (13).

Fluorodeoxyglucose (FDG) positron emission tomography (PET) imaging has emerged as an important clinical tool for cancer detection, staging, and monitoring of response and is routinely used in the clinical management of several cancer types (14, 15). FDG uptake is largely proportional to the rate of glucose metabolism, and elevated uptake is therefore a matter of enhanced glycolysis, which can be quantified (15, 16).

More than 70 years ago, Warburg discovered that malignant cells generally have increased glycolyis, even under aerobic conditions, and suggested this was a common characteristic of tumors. Subsequent reports have indicated that aerobic glycolysis is the result of a number of genetic changes (17, 18). Hypoxic cells often use enhanced glycolysis to maintain production of energy because ATP can be produced from glucose metabolism without requiring O_2. Glycolysis can be increased as much as 2-fold in acute hypoxia and is usually associated with increased expression or modified forms of glucose transporters (GLUT 1 and GLUT 3) and increased levels of hexokinase (19) as well as intracellular mitochondrial redistribution of that enzyme. Evans *et al.* (20), using Ki-67 immunocytochemistry, showed a reduction in cell proliferation in hypoxic regions of a tumor. With chronic, unabated hypoxia, cell proliferation is appreciably slowed in an effort to conserve energy and adapt to

Received 4/25/03; revised 10/6/03; accepted 10/20/03.
Grant support: NIH Grant P01-CA 42045. This work was presented at the 93rd Annual Meeting of the American Association for Cancer Research, San Francisco, California, April 2002.
The costs of publication of this article were defrayed in part by the payment of page charges. This article must therefore be hereby marked *advertisement* in accordance with 18 U.S.C. Section 1734 solely to indicate this fact.
Note: D. Mankoff was supported by NIH Grant R01-CA72064. D. Schwartz was supported by an award from the Department of Veterans Affairs, Veterans Health Administration.
Requests for reprints: Joseph Rajendran, Division of Nuclear Medicine, Box 356113, University of Washington, Seattle, Washington 98195. Phone: (206) 598-4240; Fax: (206) 598-4496; E-mail: rajan@u.washington.edu.

reduced supplies of oxygen, micronutrients, and fuel sources such as glucose (20–22). However, these changes are not uniformly expressed and can show significant heterogeneity within and between tissue types (23).

Hypoxia is widely recognized to be an independent predictor of clinical outcome (3, 24), but hypoxia in tumors is not predicted by tumor size, grade, extent of necrosis, or blood hemoglobin status. Thus, determination of tumor hypoxia carries information independent of current clinicopathological parameters and can provide important prognostic information. Nitroimidazoles are a class of electron affinic molecules that were first shown by Chapman (25) to accumulate in hypoxic cells in cultures and *in vivo*. PET imaging of tissue hypoxia ($pO_2 \leq 3$ mm Hg) using ^{18}F-labeled fluoromisonidazole (FMISO), the most widely used nitroimidazole imaging agent, was developed and validated by our group. It is a noninvasive way to localize and quantify hypoxia that can be repeated when needed (26–28).

Bentzen *et al.* (29), in evaluating the role of FMISO and FDG in identifying hypoxia in animal studies, found that FMISO was able to identify hypoxia, but they could not find a similar role for FDG. Mankoff *et al.* (12), in studying blood flow and metabolism in locally advanced breast cancer, found wide variation between the two parameters; tumors with high metabolic rates responded poorly to treatment, independent of blood flow.

Although glycolysis is increased by hypoxia, there are reasons to believe that hypoxia and glucose metabolism, as measured by FMISO and FDG PET imaging, respectively, may not follow a simple relationship. Glucose metabolism is influenced by a variety of processes other than hypoxia; for example, cellular proliferation and maintaining ion gradients will result in elevated glucose metabolism in the absence of hypoxia (30). Moreover, the poor blood supply that causes hypoxia might lead to significantly reduced delivery of nutrients such as glucose in chronic situations and hence decreased glucose uptake (31). For these reasons, we investigated the relationship of regional hypoxia and glucose metabolism by comparing FMISO and FDG uptake on PET images. The study included different tumor types, ranging from those that are frequently hypoxic (head and neck cancer and glioblastoma multiforme) to those that are less frequently hypoxic (breast cancer). Our hypothesis was that high glucose metabolism could be induced by factors other than hypoxia, and, in some hypoxic tumors, limited substrate delivery might limit increases in energy metabolism induced by hypoxia. These will result in regions that show varying patterns of discordance in the uptake of these two tracers.

Materials and Methods

Patients

A total of 49 patients were included in this review. These patients underwent pretherapy FMISO and FDG PET scans as part of several ongoing research studies and were recruited from the Veterans' Administration Puget Sound Health Care System, University of Washington Medical Center and Harborview Medical Center. Signed informed consent, as approved by the University of Washington human subjects and radiation safety committees, was obtained in all cases. Human use of [^{18}F]FMISO is covered by an Investigational New Drug approval. Patients with advanced cancer were selected for these studies to increase the chance of including tumors with significant hypoxia. FDG scans were obtained after an overnight fast (blood sugar $\leq$ 150 mg at the time of imaging). No special patient preparation was required for FMISO imaging. Patients were imaged in the supine position with head immobilization (for brain tumor and head and neck cancer patients) achieved using moldable foam. Both FMISO and FDG PET studies were obtained within a few days of each other and a few days before therapy. In addition to clinical examinations, all patients had routine staging procedures that included computed tomography or magnetic resonance scans, laryngoscopy, and biopsy as appropriate for the tumor type.

PET Imaging

All scans were performed on an Advance Tomograph (GE Medical Systems, Waukesha, WI) operating in two-dimensional high sensitivity mode with 35 imaging planes covering a 15-cm axial field of view. Performance characteristics of the tomograph have been published elsewhere (32, 33). Imaging included a 25-min transmission scan of the tumor site with a Ge-68 rotating sector source. Calibration was performed using vials containing known activities of ^{18}F imaged separately from the patient and reconstructed using the same filter as the emission images. All head and neck and torso images were reconstructed with a Hanning filter after scatter correction, resulting in a reconstructed spatial resolution of approximately 12 mm (32). Brain images were collected in three-dimensional mode and were reconstructed with a spatial resolution of 6 mm.

FDG Protocol

[^{18}F]FDG was prepared as described in Ref. 34 and injected i.v. (3.7 MBq/kg or 0.1 mCi/kg) into patients in a fasting state. Patients returned 45 min after injection and were positioned in the tomograph, and a scan of the tumor was obtained. In patients with tumors outside of the brain, an additional four to five axial fields of view (15 cm each) were obtained that included the base of skull and extended to below the liver. Emission scans (each of 7 min in duration) followed by transmission scans (3 min each) were obtained. All patients were premedicated with lorazepam as a muscle relaxant to reduce FDG uptake in skeletal muscle.

FMISO Protocol

[^{18}F]FMISO was prepared as described previously (35). Venous access lines were established in each arm, one for FMISO injection and the other for blood sampling. Patients received i.v. injection with 3.7 MBq/kg (0.1 mCi/kg) [^{18}F]FMISO [maximum 370 MBq (10 mCi)]. Data acquired from 120–140 min postinjection were reconstructed with scatter, randoms, and attenuation correction and used to determine the tumor hypoxic volume (HV) as described below. These images were reconstructed with the same software and filter size used for FDG. During emission tomography, four venous blood samples were obtained at intervals of 5 min. Whole blood

samples of 1 ml each were counted in a Cobra multichannel gamma well counter (Packard Corp. Meriden, CT) that is calibrated each week in units of cpm/μCi. Blood activity was averaged and then expressed as μCi/ml, decay corrected to time of injection.

Image Analysis

FDG. Images were directly processed to provide a maximum standardized uptake value [SUV_{max} = maximum tissue activity (μCi/ml)/injected dose (mCi/kg)] for the tumor volume. Conventional images (computed tomography, magnetic resonance) were used to delineate tumor boundaries for drawing regions of interest (ROIs). Only the primary sites of disease were included in this analysis. For each tumor, we analyzed all of the pixels in all tumor planes.

FMISO. Images were transferred to Macintosh workstations for image analysis. Generous ROIs were drawn over the entire tumor volume. All imaging planes containing tumor were analyzed. Data initially available as counts/pixel were decay corrected to the time of injection and converted to μCi/ml tissue for each pixel in the selected ROI. Because the blood values were also expressed as μCi/ml, this allowed a pixel-by-pixel calculation of tissue:blood (T:B) activity ratio for all image planes. The number of pixels in the tumor volume with a T:B ratio $\geq$ 1.2, indicating significant hypoxia, was determined and converted to ml units to measure the HV. Because FMISO has a partition coefficient of almost unity, in normal oxygenated tissues the concentrations in tissue and blood are essentially identical. The cutoff ratio of 1.2 was based on T:B ratios measured previously with the GE Advance tomograph in normal human brain and muscle, where >90% of the values fall below 1.1 (36). This very simple model analysis is one of the strengths of the FMISO study.

Regional Correlation of FDG and FMISO Uptake. For the pixel-by-pixel comparison, the FMISO and FDG scans were coregistered using software developed by Minoshima *et al.* (37). A ROI was drawn over the tumor regions in each slice of the FDG scan where tumor uptake was visualized. Correlative images (magnetic resonance, computed tomography) were used as necessary to aid in the delineation of tumor boundaries. The values were scaled to the maximum pixel for each anatomical image data set to provide unitless values with a maximum of 1. The ROI was mapped to the coregistered FMISO T:B image, and the T:B ratio was extracted for each pixel within the ROI. The coregistration and mapping procedure allowed direct comparison of pixel values in the FMISO and FDG images. Pixel-wise pairs of FDG SUV and FMISO T:B values were transferred to an Excel spread sheet (Microsoft Corp., Redmond, WA) for correlation analysis.

Statistical Analysis

FMISO and FDG uptake was investigated in a global manner and by analyzing pixel-wise correlations. The following image parameters were used in the analyses: FDG – SUV and SUV_{max}; FMISO – HV and T:B and $T:B_{max}$. Correlation between FDG and FMISO uptake was analyzed in two ways, globally (using SUV_{max} and HV) and on a pixel basis (with SUV and T:B ratio). Spearman rank correlation was also used to test for correlation. The statistical significance of differences between these measures was analyzed using the Kruskal-Wallis test. The relationship between FMISO and FDG uptake was investigated using the separate median values as the cutoff for HV and T:B ratio.

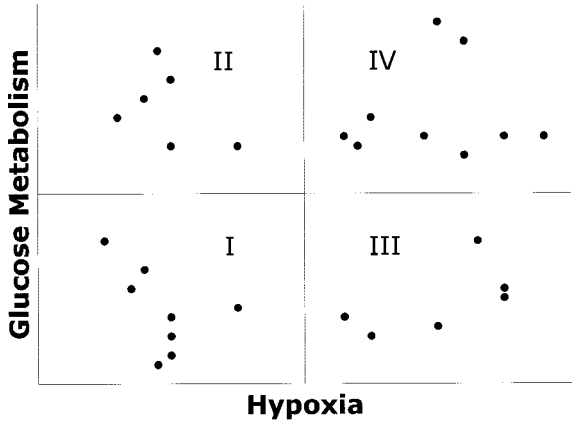

Fig. 1 Hypothetical illustration showing the possible scenarios in the correlation between hypoxia and glucose metabolism. Group I, low glucose metabolism and low hypoxia; group II, low hypoxia and high glucose metabolism; group III, high hypoxia and high glucose metabolism; group IV, high hypoxia and low glucose metabolism.

We hypothesized that the correlation between FMISO and FDG uptake would result in four possible scenarios (Fig. 1): group I, low degree of hypoxia and low glucose metabolism; group II, low degree of hypoxia but high glucose metabolism; group III, high degree of hypoxia and high glucose metabolism; and group IV, high degree of hypoxia but low level of glucose metabolism. We analyzed our data based on this fundamental hypothesis, looking for trends in the frequency of distribution of correlations in each group.

Results

The 49 previously untreated patients analyzed for this study all had biopsy proven malignancies at the time of imaging. Head and neck cancer patients had a median age of 57 years (range, 47–79 years), and a T_1 (3 patients), T_2 (5 patients), T_3 (7 patients), or T_4 (11 patients) primary tumor. Soft tissue sarcoma patients had a median age of 41 years (range, 25–72 years) with a mean tumor volume of 253 ml (range, 23–1742 ml); breast cancer patients had a median age of 45 years (range, 32–66 years), and all had stage IV disease; and glioblastoma multiforme patients had a median age of 50 years (range, 31–65 years). Only pretherapy scans were used for these analyses. Examples of patient studies, showing corresponding planes of FDG and FMISO images in axial projection, are given in Figs. 2, *A*–*D*.

Details of results for the FMISO and FDG data comparisons are given in Table 1. Statistical associations between FMISO (HV and $T:B_{max}$) and FDG SUV_{max} uptake are tabulated. When the whole tumor images were compared, correlation coefficients between SUV_{max} and HV were 0.63 for head and neck cancer, 0.47 for breast cancer, 0.38 for glioblastoma

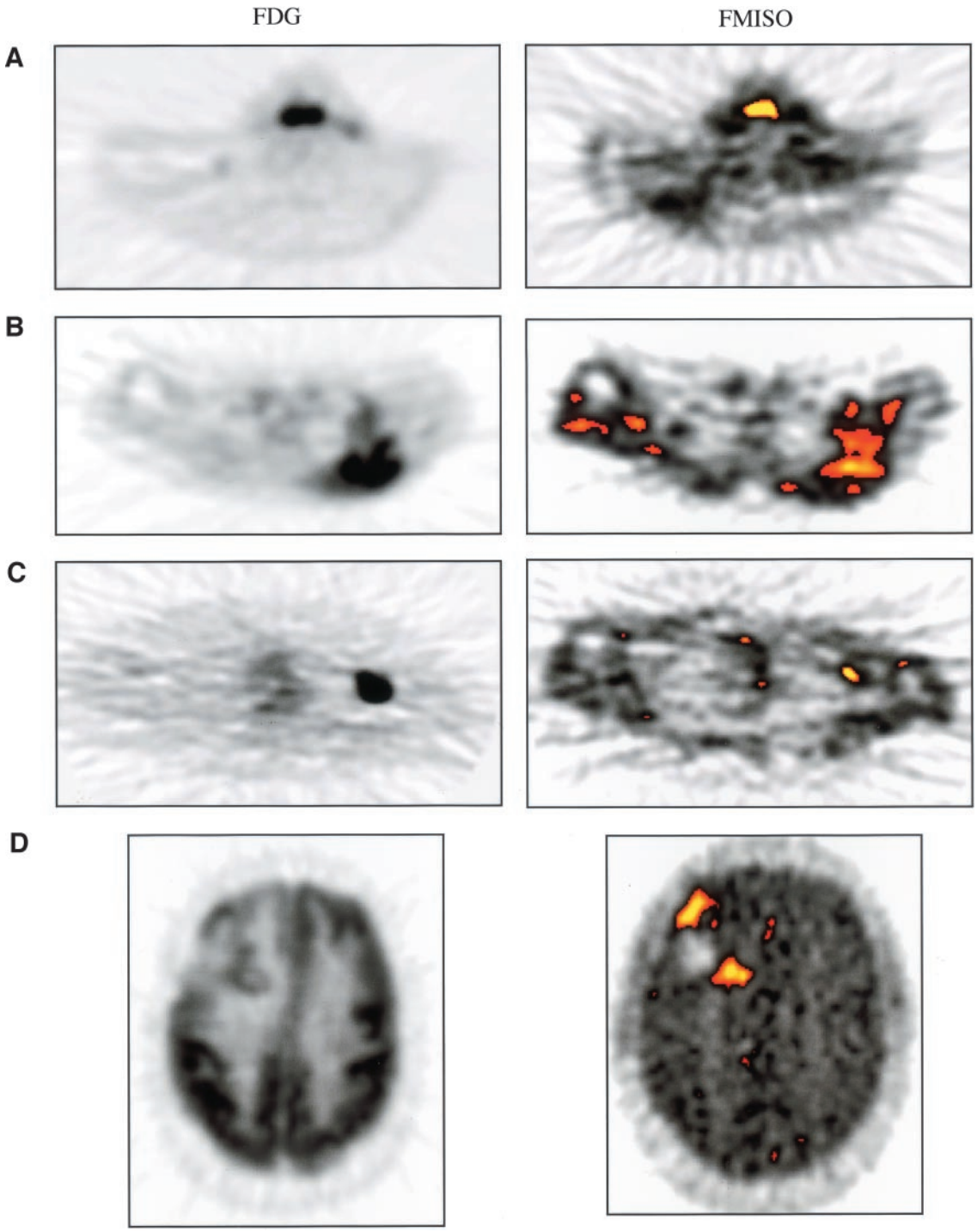

Fig. 2 Image examples for each tumor type analyzed. A representative fluorodeoxyglucose image is on the *left*, and a fluoromisonidazole image is on the *right*. *A*, patient with laryngeal cancer; *B*, patient with liposarcoma of the left posterior shoulder; *C*, patient with axillary metastases from left breast cancer; *D*, patient with glioblastoma of the right frontal region.

Table 1 FMISO[a] and FDG PET correlation data analyses for four tumor types

	Head & Neck	Sarcoma	Breast cancer	Brain tumor	Overall
No. of patients	26	11	7	5	49
$T:B_{max}$	1.54 (0.88–2.4)	1.46 (1.1–2.1)	1.52 (0.93–2.6)	2.43 (1.7–2.9)	
HV	13.03 (0–68.6)	19.2 (0–61.4)	18 (0–97.7)	20.2 (6.3–43.3)	
FDG SUV_{max}	10.9 (2.9–25.4)	8.9 (2.2–40.3)	11.7 (2–34.2)	11.9 (8.7–20.8)	
Correlation (*r*)	0.63 (0.19–0.86)	0.32 (−0.46–0.72)	0.47 (0.31–0.60)	0.38 (0.05–0.69)	
Spearman (rho)	0.41	0.24	0.21	0.5	0.241
(*P*)	0.038	0.45	0.63	0.368	0.0036[b]

[a] FMISO, fluoromisonidazole; FDG, fluorodeoxyglucose; PET, positron emission tomography; HV, hypoxic volume; SUV_{max}, maximum standardized uptake value; $T:B_{max}$, maximum tissue:blood ratio.
[b] Kruskal-Wallis *P*.

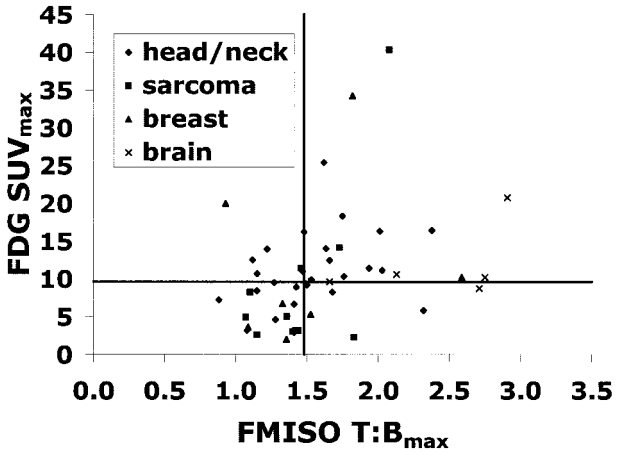

Fig. 3 Correlation between fluoromisonidazole (tissue:$blood_{max}$) and fluorodeoxyglucose for four tumor types using the median value (tissue:$blood_{max}$ = 1.48; fluorodeoxyglucose maximum standardized uptake value = 9.6) as the cutoff for analysis.

multiforme, and 0.32 for soft tissue sarcoma. Table 1 also reports Spearman correlations between the overall tumor FDG quantitation (SUV_{max}) and its HV. Overall, the correlation was small ($r = 0.24$) but nonetheless significant, with a P of <0.005. When the four tumor types are analyzed separately, there is little evidence to support an association between FDG and FMISO in any tumor type, apart from the head and neck tumors, where the nominal P was 0.038. Figs. 3 and 4 show the relationship between FDG SUV_{max} and FMISO distribution relative to median values for both HV and $T:B_{max}$. Tables 2 and 3 show the distribution of correlation based on tracer uptake.

Table 1 also reports the average pixel-by-pixel correlations observed within each tumor type. All of these average correlations are positive and are highly significant. There is clear evidence of linear association between FMISO and FDG on a pixel-by-pixel basis. However, the strength of this association varies across the tumor types with the ordering sarcoma < brain < breast < head and neck. In fact, the differences between average correlations within the tumor types are highly significant ($P < 0.005$) using the rank-based Kruskal-Wallis test.

Our results (Tables 2 and 3) indicate that all of the possible scenarios (see Figs. 3 and 4) of the relationship between FMISO and FDG in our hypothesis (Fig. 1) can occur in tumors, although groups I (low degree of hypoxia and low glucose metabolism) and III (high degree of hypoxia and high glucose metabolism) show the expected preponderance. The presence of distribution in the other groups [II (low degree of hypoxia but high glucose metabolism) and IV (high degree of hypoxia but low level of glucose metabolism)] is explained by enhanced glycolysis due to factors other than hypoxia and the lack of enhanced glycolysis even in the presence of significant hypoxia, respectively. Hypoxia is heterogeneously distributed within a tumor (38).

Discussion

Hypoxia can be a significant problem in the management of many solid tumors (3). Hypoxia-inducible factor 1α, which is overexpressed in response to hypoxia, is the primary transcription factor mediating a number of physiological and biological changes that include aerobic glycolysis and slowing of proliferation (39). This study was prompted by the greater degree of variation in FMISO and FDG uptake in several tumor types seen on PET scanning. Whereas it is reasonable to anticipate that hypoxia results in increased glycolysis, the results in our study indicate that there can be a wide variation in these two phenomena.

We analyzed the uptake patterns of these two tracers (FMISO and FDG) in two different ways: (*a*) global measures (HV and SUV_{max}); and (*b*) pixel analysis (SUV and $T:B_{max}$)

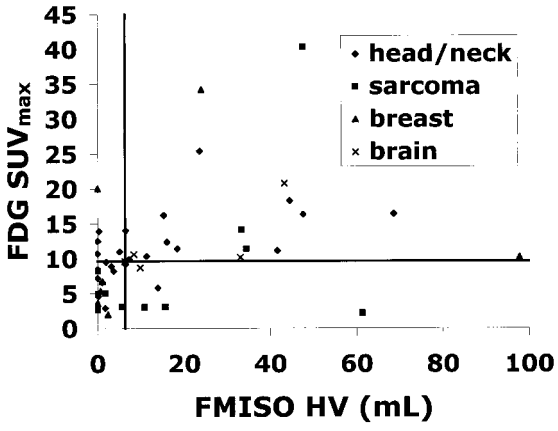

Fig. 4 Correlation between fluoromisonidazole (hypoxic volume) and fluorodeoxyglucose maximum standardized uptake value for four tumor types using the median value (hypoxic volume = 3.7; fluorodeoxyglucose maximum standardized uptake value = 9.6) as the cutoff for analysis.

using all of the pixels in the delineated tumor. Visual interpretation of these graphs showed different correlation between the global uptake of the two tracers for the various tumor types. However, because the ability to respond to hypoxia is tissue type dependent and genetically determined, the other traits might be exhibited in some situations (17).

We analyzed the global correlation between FMISO and FDG for all tumor types as summarized in Table 1. The maximum T:B ratio of FMISO uptake is nearly identical in different tumor types, whereas HV shows variation according to the tumor type. Our previous analysis of soft tissue sarcomas did not show an association between tumor volume and HV (28).

Using identical ROIs on coregistered PET images, our pixel-by-pixel analyses of these images showed only a marginally significant spatial correlation in the uptake of the two tracers. There is wide variation among tumor types (Table 1). This wide variation in uptake can be attributed to the functional and biochemical heterogeneity seen in hypoxic tissues (20). Within a tumor, oxygenation varies, ranging from well-perfused and oxygenated regions to areas that are underperfused and severely hypoxic. Existence of a mixture of acute and chronic hypoxia within a tumor is likely to be a significant factor in causing this heterogeneity (40). This is clearly seen in our patients with sarcoma, who show the least correlation between FMISO and FDG uptake. The discordance between FMISO and FDG might also be a reflection of vascularization and blood supply; tumors with poor blood supply have increased hypoxia but also have reduced glycolysis as a result of decreased supply of the nutrients (41).

Our study demonstrates heterogeneity in hypoxia and in energy metabolism and that the discordance between the uptake of FMISO and FDG does not appear to be a function of the tumor size, as seen in our analysis of a cohort of patients with soft tissue sarcomas (28). If that (tumor size) were the case, soft tissue sarcomas would be expected to show a greater degree of heterogeneity than head and neck cancers, which are relatively smaller. On the contrary, we noted heterogeneity and discordance in different cancer types, indicating that this phenomenon is ubiquitous in solid tumors and likely reflects the genetic response to hypoxic stress.

Similarly, if there were a simple mechanistic relationship between FMISO and FDG uptake, our pixel-by-pixel analyses would have indicated a higher correlation. However, this was not the case. FDG uptake is a function of many factors such as microvasculature, GLUT, hexokinase expression, and proliferation rate (22). FDG uptake has been correlated with aggressiveness of tumors and shown to be an indicator of poor prognosis in many different tumor types (12, 42–45). Tolerance to chronic hypoxia is a hallmark of higher organisms, in an effort to adapt for times of insufficient supply of oxygen and glucose (46). Bioenergetic adaptations can vary in tumor cells exposed to chronic depletion of oxygen. Our study clearly indicates that there can be a wide variation in the relationship between hypoxia and energy metabolism and all four possible scenarios can exist in tumors, a fact that needs to be considered in the clinical and imaging characterization of tumor biology and in treatment.

The presence of widespread heterogeneity in a tumor would indicate that hypoxia is diffuse throughout the tumor and that response to hypoxia will be equally widespread and varying. A diffuse hypoxic process indicates a generalized response to hypoxic stress with associated biological changes and aggressive behavior and hence with poor prognosis. On the other hand, a lesser degree of spatial heterogeneity in hypoxia might mean a more localized and well-demarcated process. This information on the biology of tumors will also have implications on treatment selection. Whereas the former requires a more general or systemic approach such as a hypoxic cell cytotoxin (*e.g.*, tirapazamine) to solve the problem of hypoxia (47), a more focal hypoxia might benefit from a local/regional approach [*e.g.*, radiation dose escalation (48)].

Our study is limited by the small number of patients. However, we have included in our analysis several tumor types differing in degrees of hypoxia and several corresponding planes on both FMISO and FDG images. This provides us enough statistical advantage. Although significant heterogeneity in the uptake of these two tracers exists, it is impossible to look at any degree of variation in the uptake between individual tumor cells using current PET technology. However, it is apparent that hypoxia-induced changes in a group of cells, rather than in an individual cell, are clinically and radiobiologically more significant; an analysis of the variation between individual cells is not likely to result in any advantage for treatment using current technologies. PET FMISO imaging will likely provide a "road map" for tissue sampling in characterizing biomarker expression. Whereas FDG uptake might indicate the presence of hypoxia (49, 50), it should not be considered as a surrogate marker for hypoxia (51). Thus, using both FMISO and FDG appears to be beneficial in the evaluation of solid tumors. Additional patient studies that include other tumor types are needed before more definitive conclusions can be reached.

Table 2 Distribution of correlative uptake values based on tracer uptake relative to corresponding median values for FDG[a] SUV_{max} and FMISO HV

+ and − indicate above and below the median values.

	FMISO−	FMISO+
FDG+	5	22
FDG−	17	5

[a] FDG, fluorodeoxyglucose; SUV_{max}, maximum standardized uptake value; FMISO, fluoromisonidazole; HV, hypoxic volume.

Table 3 Distribution of correlative uptake values based on tracer uptake FDG[a] SUV_{max} and FMISO $T:B_{max}$

+ and − indicate above and below the median values.

	FMISO−	FMISO+
FDG+	6	22
FDG−	15	6

[a] FDG, fluorodeoxyglucose; SUV_{max}, maximum standardized uptake; FMISO, fluoromisonidazole; $T:B_{max}$, maximum tissue:blood ratio.

Acknowledgments

We thank the following for their help: Jeff Scharnhorst (RN), patient care coordinator and database manager; and all nuclear medicine

technologists, radiochemists, and physicists in the Division of Nuclear Medicine.

References

1. Hockel M, Schlenger K, Knoop C, Vaupel P. Oxygenation of carcinomas of the uterine cervix: evaluation by computerized O_2 tension measurments. Cancer Res 1991;51:6098–102.
2. Vaupel P, Schlenger K, Knoop C, Hockel M. Oxygenation of human tumors: evaluation of tissue oxygen distribution in breast cancers by computerized O_2 tension measurements. Cancer Res 1991;51:3316–22.
3. Brown MJ. The hypoxic cell: a target for selective cancer therapy. Eighteenth Bruce F. Cain Memorial Award Lecture. Cancer Res 1999; 59:5863–70.
4. Teicher BA. Hypoxia and drug resistance. Cancer Metastasis Rev 1994;13:139–68.
5. Sutherland RM. Tumor hypoxia and gene expression: implications for malignant progression and therapy. Acta Oncol 1998;37:567–74.
6. Adam M, Gabalski EC, Bloch DA, et al. Tissue oxygen distribution in head and neck cancer patients. Head Neck 1999;21:146–53.
7. Rasey JS, Koh WJ, Evans ML, et al. Quantifying regional hypoxia in human tumors with positron emmision tomography of [^{18}F]fluoromisonidazole: a pretherapy study of 37 patients. Int J Radiat Biol Phys 1996;36:417–28.
8. Brizel DM, Sibley GS, Prosnitz LR, Scher RL, Dewhirst MW. Tumor hypoxia adversely affects the prognosis of carcinoma of the head and neck. Int J Radiat Oncol Biol Phys 1997;38:285–9.
9. Brizel DM, Rosner GL, Harrelson J, Prosnitz LR, Dewhirst MW. Pretreatment oxygenation profiles of human soft tissue sarcomas. Int J Radiat Oncol Biol Phys 1994;30:635–42.
10. Nordsmark M, Loncaster J, Chou SC, et al. Invasive oxygen measurements and pimonidazole labeling in human cervix carcinoma. Int J Radiat Oncol Biol Phys 2001;49:581–6.
11. Knowles HJ, Harris AL. Hypoxia and oxidative stress in breast cancer. Hypoxia and tumourigenesis. Breast Cancer Res 2001;3:318–22.
12. Mankoff DA, Dunnwald LK, Gralow JR, et al. Blood flow and metabolism in locally advanced breast cancer: relationship to response to therapy. J Nucl Med 2002;43:500–9.
13. Valk P, Mathis C, Prados M, Gilbert J, Budinger T. Hypoxia in human gliomas: demonstration by PET with flouorine-18-fluoromisonidazole. J Nucl Med 1992;33:2133–7.
14. Eary JF, Conrad EU. Positron emission tomography in grading soft tissue sarcomas. Semin Musculoskelet Radiol 1999;3:135–8.
15. Stokkel MP, ten Broek FW, van Rijk PP. The role of FDG PET in the clinical management of head and neck cancer. Oral Oncol 1998;34: 466–71.
16. Visser FC. Imaging of cardiac metabolism using radiolabelled glucose, fatty acids and acetate. Coron Artery Dis 2001;12(Suppl 1):S12–8.
17. Semenza GL, Artemov D, Bedi A, et al. "The metabolism of tumours": 70 years later. Novartis Found Symp 2001;240:251–60; discussion 260–254.
18. Racker E, Spector M. Warburg effect revisited: merger of biochemistry and molecular biology. Science (Wash. DC) 1981;213: 303–7.
19. Burgman P, Odonoghue JA, Humm JL, Ling CC. Hypoxia-induced increase in FDG uptake in MCF7 cells. J Nucl Med 2001; 42:170–5.
20. Evans SM, Hahn SM, Magarelli DP, Koch CJ. Hypoxic heterogeneity in human tumors: EF5 binding, vasculature, necrosis, and proliferation. Am J Clin Oncol 2001;24:467–72.
21. Clavo AC, Wahl RL. Effects of hypoxia on the uptake of tritiated thymidine, L-leucine, L-methionine and FDG in cultured cancer cells. J Nucl Med 1996;37:502–6.
22. Bos R, van Der Hoeven JJ, van Der Wall E, et al. Biologic correlates of (18)fluorodeoxyglucose uptake in human breast cancer measured by positron emission tomography. J Clin Oncol 2002;20:379–87.
23. Walenta S, Snyder S, Haroon ZA, et al. Tissue gradients of energy metabolites mirror oxygen tension gradients in a rat mammary carcinoma model. Int J Radiat Oncol Biol Phys 2001;51:840–8.
24. Rasey JS, Hofstrand PD, Chin LK, Tewson TJ. Characterization of [^{18}F]fluoroetanidazole, a new radiopharmaceutical for detecting tumor hypoxia. J Nucl Med 1999;40:1072–9.
25. Chapman JD. The detection and measurement of hypoxic cells in solid tumors. Cancer (Phila.) 1984;54:2441–9.
26. Rasey JS, Koh WJ, Grierson JR, Grunbaum Z, Krohn KA. Radiolabelled fluoromisonidazole as an imaging agent for tumor hypoxia. Int J Radiat Oncol Biol Phys 1989;17:985–91.
27. Koh WJ, Rasey JS, Evans ML, et al. Imaging of hypoxia in human tumors with [F-18]fluoromisonidazole. Int J Radiat Oncol Biol Phys 1992;22:199–212.
28. Rajendran JG, Wilson D, Conrad EU, et al. F-18 FMISO and F-18 FDG PET imaging in soft tissue sarcomas: correlation of hypoxia, metabolism and VEGF expression Eur J Nucl Med 2003;30:695–704.
29. Bentzen L, Keiding S, Horsman MR, et al. Feasibility of detecting hypoxia in experimental mouse tumours with 18F-fluorinated tracers and positron emission tomography: a study evaluating [^{18}F]fluoro-2-deoxy-D-glucose. Acta Oncol 2000;39:629–37.
30. Spence AM, Muzi M, Graham MM, et al. Analysis of the deoxyglucose lumped constant in human malignant gliomas. Ann Neurol 1991;30:271–2.
31. Kallinowski F, Schlenger KH, Kloes M, Stohrer M, Vaupel P. Tumor blood flow: the principal modulator of oxidative and glycolytic metabolism, and of the metabolic micromilieu of human tumor xenografts in vivo. Int J Cancer 1989;44:266–72.
32. Lewellen TK, Kohlmeyer SG, Miyaoka RS, et al. Investigation of the count rate performance of the General Electric Advance positron emission tomograph. IEEE Trans Nucl Sci 1995;42:1051–7.
33. DeGrado TR, Turkington TG, Williams JJ, et al. Performance characteristics of a whole-body PET scanner. J Nucl Med 1994;35: 1398–1406.
34. Hamacher K, Coenen HH, Stocklin G. Efficient stereospecific synthesis of no-carrier-added 2-[^{18}F]-fluoro-2-deoxy-D-glucose using aminopolyether supported nucleophilic substitution. J Nucl Med 1986;27: 235–8.
35. Grierson JR, Link JM, Mathis CA, Rasey JS, Krohn KA. Radiosynthesis of of fluorine-18 fluoromisonidazole. J Nucl Med 1989;30: 343–50.
36. Rajendran JG, Krohn KA. Imaging tumor hypoxia. In: Bailey DL, Townsend DW, Valk PE, Maisey MN, editors. Positron emission tomography, principles and practice. London: Springer Verlag; 2002. p. 689–95.
37. Minoshima S, Berger KL, Lee KS, Mintun MA. An automated method for rotational correction and centering of three-dimensional functional brain images. J Nucl Med 1992;33:1579–85.
38. Rajendran J, Lanell P, Schwartz DS, et al. [F-18] FMISO PET hypoxia imaging in head and neck cancer: heterogeneity in hypoxia. Primary tumor vs lymph nodal metastases J Nucl Med 2002;43:73P.
39. Pedersen MW, Holm S, Lund EL, Hojgaard L, Kristjansen PE. Coregulation of glucose uptake and vascular endothelial growth factor (VEGF) in two small-cell lung cancer (SCLC) sublines in vivo and in vitro. Neoplasia 2001;3:80–7.
40. Denekamp J, Dasu A. Inducible repair and the two forms of tumour hypoxia: time for a paradigm shift. Acta Oncol 1999;38:903–18.
41. Erecinska M, Nelson D, Deas J, Silver IA. Limitation of glycolysis by hexokinase in rat brain synaptosomes during intense ion pumping. Brain Res 1996;726:153–9.
42. Eary JF, O'Sullivan F, Powitan Y, et al. Sarcoma tumor FDG uptake measured by PET and patient outcome: a retrospective analysis. Eur J Nucl Med Mol Imaging 2002;29:1149–54.
43. Kitagawa Y, Sano K, Nishizawa S, et al. FDG-PET for prediction of tumour aggressiveness and response to intra-arterial chemotherapy

and radiotherapy in head and neck cancer. Eur J Nucl Med Mol Imaging 2003;30:63–71.

44. Spence AM, Muzi M, Krohn KA. Molecular imaging of regional brain tumor biology. J Cell Biochem Suppl 2002;39:25–35.

45. Oshida M, Uno K, Suzuki M, et al. Predicting the prognoses of breast carcinoma patients with positron emission tomography using 2-deoxy-2-fluoro[^{18}F]-D-glucose. Cancer (Phila.) 1998;82:2227–34.

46. Esumi H, Izuishi K, Kato K, et al. Hypoxia and nitric oxide treatment confer tolerance to glucose starvation in a 5′-AMP-activated protein kinase-dependent manner. J Biol Chem 2002;277:32791–8.

47. Brown JM. Exploiting the hypoxic cancer cell: mechanisms and therapeutic strategies. Mol Med Today 2000;6:157–62.

48. Chao KS, Low DA, Perez CA, Purdy JA. Intensity-modulated radiation therapy in head and neck cancers: the Mallinckrodt experience. Int J Cancer 2000;90:92–103.

49. Pauwels EK, Ribeiro MJ, Stoot JH, et al. FDG accumulation and tumor biology. Nucl Med Biol 1998;25:317–22.

50. Clavo AC, Brown RS, Wahl RL. Fluorodeoxyglucose uptake in human cancer cell lines is increased by hypoxia. J Nucl Med 1995;36: 1625–32.

51. Dehdashti F, Grigsby PW, Mintun MA, et al. Assessing tumor hypoxia in cervical cancer by positron emission tomography with (60)Cu-ATSM: relationship to therapeutic response–a preliminary report. Int J Radiat Oncol Biol Phys 2003;55:1233–8.